Title

Lentiviral hematopoietic stem cell gene therapy for X-linked severe combined immunodeficiency

Journal

Science Translational Medicine, 8(335)

ISSN

1946-6234

Authors

De Ravin, Suk See
Wu, Xiaolin
Moir, Susan
et al.

Publication Date

2016-04-20

DOI

10.1126/scitranslmed.aad8856

Peer reviewed

CORRECTED 1 JUNE 2016; SEE ERRATUM

GENE THERAPY

Lentiviral hematopoietic stem cell gene therapy for X-linked severe combined immunodeficiency

Suk See De Ravin,[1]* Xiaolin Wu,[2] Susan Moir,[3] Lela Kardava,[3] Sandra Anaya-O'Brien,[1] Nana Kwatemaa,[1] Patricia Littel,[1] Narda Theobald,[1] Uimook Choi,[1] Ling Su,[2] Martha Marquesen,[1] Dianne Hilligoss,[1] Janet Lee,[1] Clarissa M. Buckner,[3] Kol A. Zarember,[1] Geraldine O'Connor,[4] Daniel McVicar,[4] Douglas Kuhns,[2] Robert E. Throm,[5] Sheng Zhou,[5] Luigi D. Notarangelo,[6] I. Celine Hanson,[7] Mort J. Cowan,[8] Elizabeth Kang,[1] Coleen Hadigan,[3] Michael Meagher,[5] John T. Gray,[9] Brian P. Sorrentino,[5†] Harry L. Malech[1*†]

X-linked severe combined immunodeficiency (SCID-X1) is a profound deficiency of T, B, and natural killer (NK) cell immunity caused by mutations in *IL2RG* encoding the common chain (γc) of several interleukin receptors. Gamma-retroviral (γRV) gene therapy of SCID-X1 infants without conditioning restores T cell immunity without B or NK cell correction, but similar treatment fails in older SCID-X1 children. We used a lentiviral gene therapy approach to treat five SCID-X1 patients with persistent immune dysfunction despite haploidentical hematopoietic stem cell (HSC) transplant in infancy. Follow-up data from two older patients demonstrate that lentiviral vector γc transduced autologous HSC gene therapy after nonmyeloablative busulfan conditioning achieves selective expansion of gene-marked T, NK, and B cells, which is associated with sustained restoration of humoral responses to immunization and clinical improvement at 2 to 3 years after treatment. Similar gene marking levels have been achieved in three younger patients, albeit with only 6 to 9 months of follow-up. Lentiviral gene therapy with reduced-intensity conditioning appears safe and can restore humoral immune function to posthaploidentical transplant older patients with SCID-X1.

INTRODUCTION

Haploidentical hematopoietic stem cell transplantation (HSCT) without conditioning for treatment of X-linked severe combined immunodeficient (SCID-X1) infants achieves ≥70% long-term survival. However, although donor T cells engraft and are functional, two thirds of such patients lack B and natural killer (NK) cell reconstitution, which may ultimately lead to progressive clinical deterioration (*1*–*3*). Gamma-retroviral (γRV) gene therapy without conditioning effectively corrects the T cell lineage with no transduced B or NK cells in SCID-X1 infants (*4*) but fails in posthaploidentical HSCT older children, possibly due to age-related thymic damage (*5*, *6*).

Leukemias occurred in γRV gene therapy for SCID-X1, Wiskott-Aldrich syndrome (WAS), and chronic granulomatous disease (CGD) attributable to preferential integration near oncogenes (*7*–*10*). Adding a self-inactivating element (SIN) in γRV gene therapy for SCID-X1 infants resulted in a similar integration pattern as earlier γRV trials, although less clustering near oncogenes is observed at 38-month follow-up (*11*). Unlike murine γRV (mγRV), lentiviral vectors (LVs) do not preferentially integrate near enhancers and promoters, and successful SIN-LV gene therapy using marrow conditioning of WAS and metachromatic leukodystrophy (MLD) (*12*, *13*) suggests that SIN-LV may be applicable to SCID-X1.

Here, we used a codon-optimized SIN-LV (Cl20-i4-EF1α-hγcOPT), where the elongation factor 1α (EF1α) core promoter element drives production of the common γ chain (γc) with an additional safety feature of a 400–base pair (bp) chicken β-globin chromatin insulator element (cHS4) (fig. S10) (*14*, *15*). Preclinical studies demonstrated safety and efficacy in animal models (*16*, *17*). We report successful SIN-LV gene therapy of older SCID-X1 patients who had substantial immune and functional problems after previous haploidentical HSCT. Novel features of our clinical trial include the first use of SIN-LV to treat SCID-X1, the first use of busulfan conditioning for gene therapy of SCID-X1, and the first use of SIN-LV in patients, to be manufactured from a stable LV producer cell line (*18*). Reduced-intensity conditioning has proven to be beneficial in gene therapy for adenosine deaminase (ADA) deficiency SCID (ADA-SCID), including the development of gene-marked B and NK cells (*19*, *20*).

RESULTS

Patient characteristics

Five male patients with SCID-X1, aged 23, 22, 7, 16, and 10 years [patients 1 to 5 (P1 to P5)], with persistent disease after one or more haploidentical HSCT (Table 1), were treated in a phase 1/2 clinical trial. This report describes the course of P1 and P2 through 36 and 24 months and P3 to P5 through 9, 6, and 6 months after autologous SIN-LV (EF1α-hγcOPT)–transduced CD34$^+$ HSC transplant, with a total of 6 mg of busulfan/kg, intravenously, for conditioning. Busulfan levels were drawn on day 1 after the first 3 mg of busulfan/kg dose and ranged from 2519.6 to 4528.9 min*μM (Table 1). Results of the AUC levels were not available in time to allow dose adjustment. The patients recovered their absolute cell numbers without the need of blood product support for discharge within 1 month (fig. S2) and were monitored per protocol schedule (table S1).

[1]Laboratory of Host Defenses, National Institute of Allergy and Infectious Diseases (NIAID), National Institutes of Health (NIH), Bethesda, MD 20892, USA. [2]Cancer Research Technology Program, Leidos Biomedical Research Inc., Frederick National Laboratory for Cancer Research, Frederick, MD 21702, USA. [3]Laboratory of Immunoregulation, NIAID, NIH, Bethesda, MD 20892, USA. [4]Cancer and Inflammation Program, National Cancer Institute Frederick, Frederick, MD 21702, USA. [5]Department of Hematology, St. Jude Children's Research Hospital, Memphis, TN 38105, USA. [6]Division of Immunology, Boston Children's Hospital, Harvard Medical School, Boston, MA 02115, USA. [7]Texas Children's Hospital, Houston, TX 77030, USA. [8]Department of Pediatrics, Benioff Children's Hospital, and University of California, San Francisco, San Francisco, CA, USA. [9]Audentes Therapeutics, San Francisco, CA 94101, USA.
*Corresponding author. E-mail: sderavin@niaid.nih.gov (S.S.D.R.); hmalech@niaid.nih.gov (H.L.M.)
†These authors share co-senior authorship.

Table 1. Patient characteristics and treatment. All patients received allogeneic stem cell transplant (HSCT) from haploidentical (haplo) parent donor once or repeated (booster). IL2RG, interleukin 2 receptor γ; CFU, colony-forming units; PLE, protein-losing enteropathy; IVIG, intravenous immunoglobulin; AUC, area under the curve.

	P1	P2	P3	P4	P5
IL2RG mutation	823T>G	447 delA	923C>A	c341G>A	31T>A
Age (years)	23	22	7	15	10
Prior HSCT	Haplo, booster	Haplo	Haplo, booster	Haplo	Haplo, booster
Immunophenotype	↓ T, B, NK	↓ B, NK	↓ T, B, NK	↓ T, B, NK	↓ T, B, NK
Medical problems	Norovirus, infections, PLE, IVIG	Norovirus, infections, IVIG, warts, molluscum, bronchiectasis, bronchiolitis obliterans	Norovirus, infections, PLE, IVIG, bronchiectasis, growth failure	Norovirus, infections, PLE, IVIG, bronchiectasis	Norovirus, PLE, IVIG, molluscum, bronchiectasis
Busulfan AUC (min*μM)	3603.1	4528.9	2519.6	4523.6	3096.6
$CD34^+$ cells infused ($\times 10^6$/kg)	18	16	20.4	21.7	25
Bulk CD34 in vitro CFU (%)	27	17	22	57.7	36.1
Follow-up (months)	36	24	6	3	3
Current status	Cleared norovirus, off IVIG	Cleared norovirus, off IgG supplement, fatal bronchial bleed	Stable	Stable	Stable

SIN-LV from stable producer and HSC transduction

The LV used in the study is SIN and uses an EF1α promoter to drive a codon-optimized human γc complementary DNA (cDNA), flanked by a 400-bp chicken insulator (*14*, *15*). Unlike γRV that is produced by stable cell lines, LV used for clinical gene therapy trials thus far relies on transient, four-plasmid transfections of packaging cells. The quantity of high-titer clinical-grade vector produced using this approach is generally insufficient to treat larger (adult) subjects. In contrast, the stable SIN EF1α-hγcOPT producer can make up to 150 liters of vector at 5×10^6 infectious units (iu)/ml for each production run. The downstream process and quality controls resulted in vector at 4×10^8 to 7×10^8 iu/ml as previously described (*15*, *18*).

$CD34^+$ HSCs were mobilized with granulocyte colony-stimulating factor (G-CSF) and plerixafor (*21*) and were collected by apheresis and cryopreserved. Autologous HSCs (1×10^7 to 2×10^7 $CD34^+$ HSCs/kg) were prestimulated with stem cell factor Fms-related tyrosine kinase 3 ligand (FLT-3L) and thrombopoietin (100 ng/ml) for 16 hours before two daily 7-hour transductions at a multiplicity of infection of 100 to 150 with vector concentration ~30% of culture volume (fig. S1). On day 3, transduced cells were washed and infused after confirmation of quality and safety criteria. Between 17.0 and 57.7% of colonies derived from the bulk transduced cells were gene-marked (Table 1).

Multilineage gene marking and immune reconstitution after gene therapy

Peripheral blood cells from patients were purified by density fractionation and magnetic bead–based immunoselection into lineages including polymorphonuclear cells (PMN), CD14, CD3, CD19, and NK cells (see Supplementary Materials and Methods). Gene marking was monitored over 2 to 3 years in P1 and P2 and demonstrated an increase in gene marking for all lineages tested (Fig. 1A). Myeloid marking in PMN and $CD14^+$ cells appeared by 2 weeks and stabilized by 6 months at 0.08 to 0.1 vector copy number (VCN) per cell in both P1 and P2. Vector marking of B and NK cells appeared later, but the levels exceeded those of myeloid cells at 0.30 to 0.40 and 0.56 to 0.77 VCN, respectively. T cell marking lagged until 5 to 6 months after treatment but steadily increased to 0.13 to 0.57 VCN. $CD14^+$ and B cell marking occurs early in all five patients, particularly in P4 and P5, who received relatively larger doses of corrected HSCs (Fig. 1B). Gene marking was also evident in circulating peripheral blood $CD34^+$ HSCs from P1 and P2 at 1 year and at 4 months, respectively, approaching the myeloid levels (Fig. 1A).

Emergence of gene-corrected autologous T cells

To preserve donor T cells, patients did not receive T cell–depleting agents. Autologous T cells, identified by microsatellite DNA fingerprinting chimerism analysis, increased about 10 months after treatment (Fig. 1C), corresponding to the increase in T cell vector marking and T cell numbers in P1 (Fig. 1D). In P2, increased gene marking in T cells with concomitant increased autologous T cell chimerism without substantial changes in his total number of T cells likely reflected a replacement of donor T cells by the autologous gene-corrected T cells (Fig. 1D). A possible explanation for the relative survival advantage of autologous gene-corrected T cells may be the better crosstalk between autologous T cells and the other immune cells or the constitutive expression of γc, although no increases in the expression of γc or its downstream signaling component JAK3 (Janus kinase 3) were found in the earlier gene therapy trials (*22*). T cell receptor excision circles (TRECs), a measure of thymus-derived T cells, increased from <25 TREC/μg to 90 to 120 TREC/μg DNA in both P1 and P2, where the lower limit of normal range for this assay is 75 TREC/μg DNA (fig. S4). In vitro T cell functional responses to mitogenic stimulation were significantly improved after treatment (Fig. 2A). Because of a lag in the appearance of gene-marked immune cells, a less substantial increase is expected in P3 to P5 at this early stage (fig. S5).

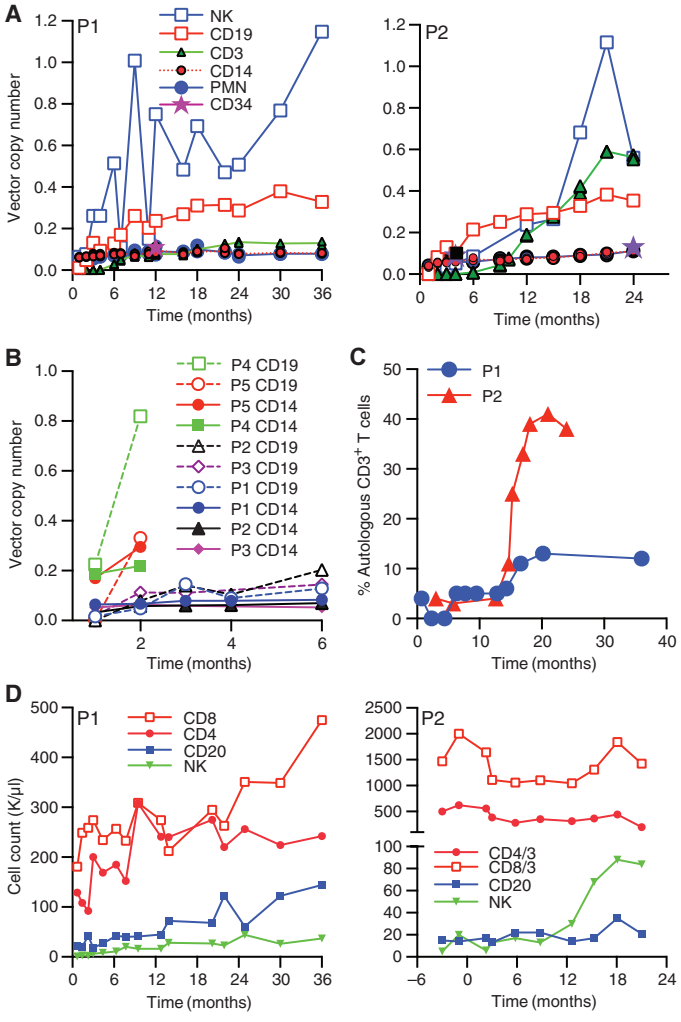

Fig. 1. Immune cell gene marking and numbers after gene therapy. (**A**) Gene marking in sorted cell lineages as vector copy number (VCN) per genome after treatment in P1 (to 36 months) and P2 (to 24 months). (**B**) Early gene marking in first 6 months in myeloid and B cells in P1 to P5. (**C**) Percent autologous (corrected) host cells as determined by restriction fragment length polymorphism assay of T cell chimerism. (**D**) Immune cell numbers in P1 and P2 after treatment. K/μl, thousands per cubic milliliter.

Gene-corrected transitional B cells and humoral reconstitution

Gene-corrected B cells emigrating from bone marrow first appear in peripheral blood as immature/transitional T1 ($CD10^{++}/CD21^{lo}$) B cells, which increased in P3 from 2.6% before treatment to 25% at 8 weeks after treatment (Fig. 2, B and C), subsequently differentiating into transitional T2/T3 ($CD10^{+}/CD21^{hi}$) B cells with a concomitant decrease in T1 being noted from 9 weeks (Fig. 2, B and C), consistent with previously described phenotypes (*14*, *23*). The derivation of T1 and T2/3 B cells was confirmed by gene marking in sorted B cell subsets, with VCN in T1>T2/3>naïve> myeloid for P3 to P5 (Fig. 2F). Longer follow-up in P1 and P2 demonstrated functional correction in B cells with class switching to $IgG^{+}CD27^{+}$ memory B cells (fig. S6) and normal IgG (Fig. 2D). In all patients, serum IgM increased starting about 3 months after therapy (Fig. 2E). Interpretation of IgG production in patients receiving IgG supplements is challenging, although IgM levels are not affected by IgG supplementation. Along with the early appearance of gene-marked B cells, serum IgM levels also increased early with the greatest increases seen in P1 and P4. These subjects had the largest proportion of vector-positive colonies from the CFU assay performed on the bulk transduced HSCs, especially P4, who also achieved the highest level of busulfan AUC and received the most $CD34^{+}$ cells. A diagnostic workup for monoclonal gammopathy in P1 (including positron emission tomography–computed tomography) was negative, and the increased IgM levels spontaneously declined as the IgG levels increased. Response to IL21 was demonstrated in vitro with peripheral blood cells from P1 at 6 months after therapy (Fig. 3A). Enzyme-linked immunospot (ELISpot) analysis of P1 before and after vaccination with the 2013 flu vaccine (at 12 months after therapy) demonstrated significantly increased vaccine-specific IgG^{+} B cell frequencies, as well as the total number of IgG^{+} B cells, thus confirming reconstitution of humoral immunity (Fig. 3B). Vaccine-induced responses to polio, diphtheria, tetanus, haemophilus were observed in P1 and P2, including a robust response in P1 to antirabies vaccination, a U.S. Food and Drug Administration (FDA)–approved antigen, achieving an antirabies titer of 11.3 international units/ml (>0.5 IU/ml represents acceptable response). Of note, the improved B cell responses may be attributable to the interaction of the gene-corrected B cells with either the donor T cells or the autologous gene-corrected T cells.

Gene marking in $CD3^{-}CD56^{+}$ NK cells also appeared by 2 months and doubled by 15 months for P2 (Fig. 1A). Posttherapy NK cells had features of mature NK cells similar to those observed in healthy controls (fig. S7). The increase in P2's NK cell numbers coincided with shrinkage of warts (Fig. 4A).

Clinical benefits

For P2, extensive molluscum contagiosum and disfiguring warts on both hands improved after gene therapy (Fig. 4A). Chronic (>2 years before treatment) norovirus infections in P1 and P2 were cleared within 21 months of therapy, and severe protein-losing enteropathy was resolved with normalization of albumin, and weight gain indicative of an improved nutritional state (Fig. 4, B and C). P2 entered the study with bronchiectasis with irreversible airway damage (fig. S8) complicated by severely impaired pulmonary function (<40% of normal). Worsening lung disease led to a fatal pulmonary bleed at 27 months after gene therapy.

Vector integration clonality analysis

Vector integration site analysis (VISA) of sorted blood lineages in P1 and P2, using previously described methods (*24*, *25*), identified 333,822 integration events, of which 38% were unique integration sites and most clones comprising <1% of total sites (Fig. 5A). Using the Chao estimator for species richness, we observed the greatest diversity in B cells, followed by myeloid cells, then T and NK cells (table S2) (*26*). In addition to the diversity of the integration site repertoire, our goal is to be able to detect clone(s) that may undergo any significant expansion. Oligoclonality index (*27*) may overestimate polyclonality in situations of limited library size or sample material, further described in the Supplementary Materials and Methods. To facilitate comparison of clonal expansion between samples, we determined the number of unique clones comprising the top 50% of the total clones, the unique clone index (UC_{50}) (Fig. 5A) (Supplementary Materials and Methods). UC_{50} for NK cells suggests a more limited diversity

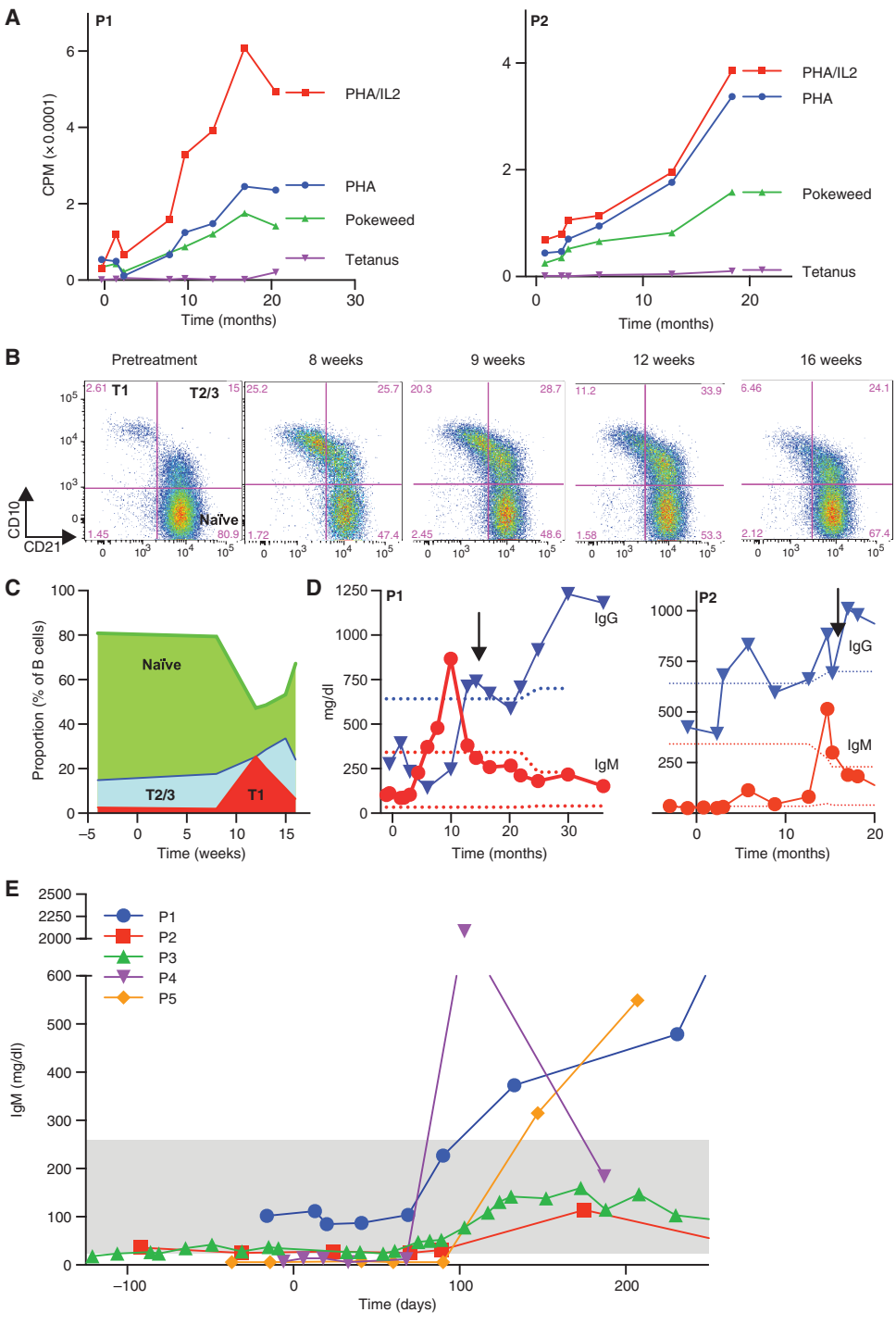

Fig. 2. Functional correction of T and B cells with SIN-LV gene therapy. (**A**) CD3 T cell proliferative responses to indicated stimuli. CPM, counts per minute; PHA, phytohemagglutinin. (**B**) Emergence of transitional T1 B cells ($CD10^{++}CD21^{lo}$) in P3 at 12 weeks, progressing to T2/3 B cells ($CD10^{+}CD21^{hi}$) by 16 weeks after gene therapy. (**C**) Changes in B cell subset profiles over time in P3. (**D**) Serum immunoglobulin M (IgM) and IgG over time in P1 and P2 after treatment. Withdrawal of supplemental IgG is indicated by the arrow. Dotted lines indicate respective normal reference ranges. (**E**) Early increases in IgM, comparing P1 to P5. (**F**) A summary of VCN in flow-sorted T1, T2/3, and naïve B cells compared to CD3 T cells from P3, P4, and P5.

F

	Vector copy number			
Month	T1	T2/3	Naïve	CD3
#3–2	0.253	0.157	0.019	0.010
#3–3	0.385	0.258	0.053	0.025
#4–3	1.350	1.106	0.751	0.021
#5–3	0.740	0.716	0.175	0.020

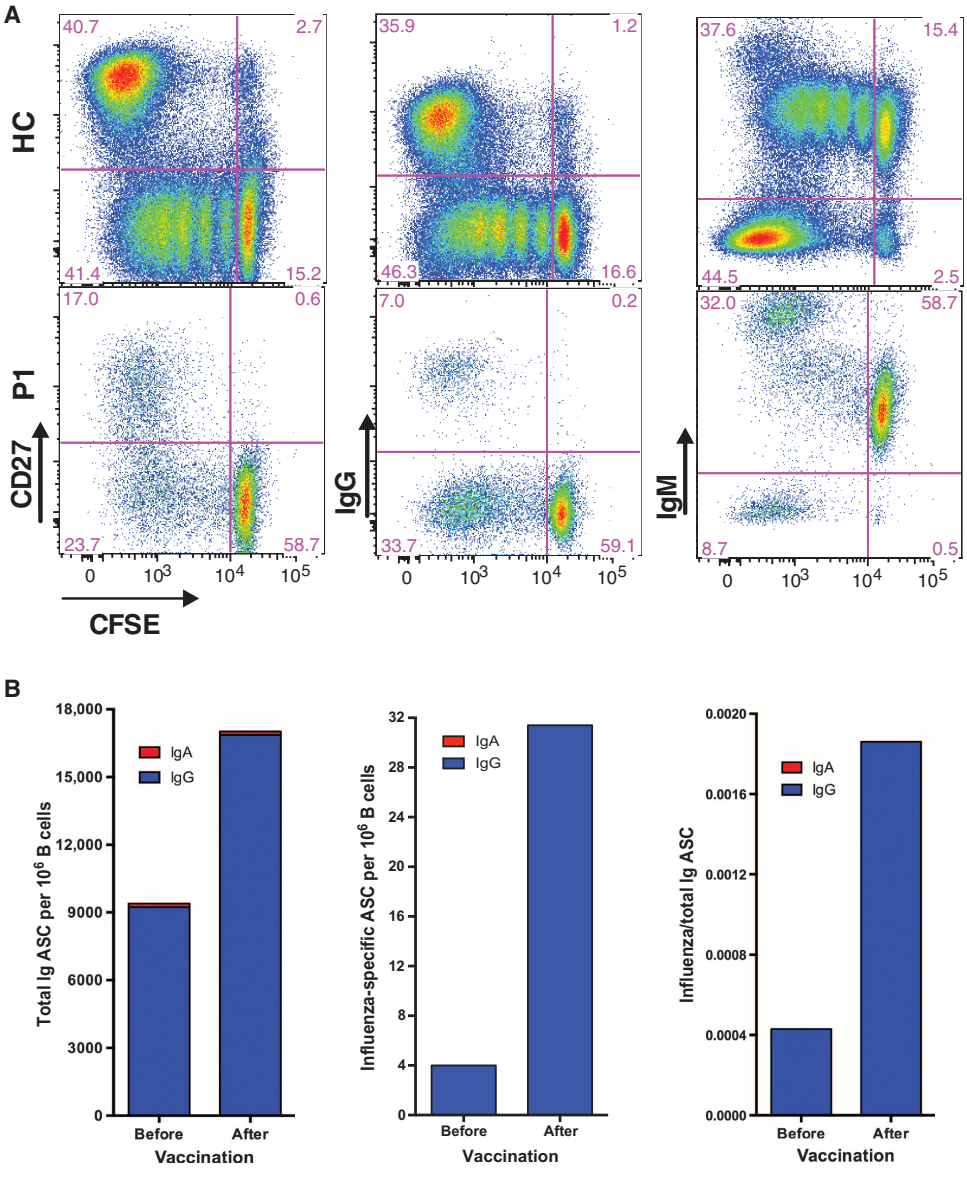

Fig. 3. Restoration of B cell signaling and specific antibody production. (**A**) B cell responses to IL21 and CD40 ligand (CD40L) stimulation. Peripheral blood mononuclear cells (PBMCs) from P1 (bottom) and a healthy control (HC, top) were stained with carboxyfluorescein diacetate succinimidyl ester (CFSE) and stimulated with IL21 and CD40L. Gated $CD3^{-}CD19^{+}$ B cells that have undergone division are shown in left upper area showing $CD27^{+}$-expressing (left panels), IgG^{+}-expressing (middle panels), and IgM^{+}-expressing (right panels) B cells. (**B**) ELISpot of P1 B cells before and after vaccination. Numbers of Ig antibody-secreting cells (ASC) (left), influenza-specific ASC per 10^6 B cells, and influenza-specific as a fraction of total Ig ASC (right) detected by ELISpot of peripheral blood B cells from P1 before and after influenza vaccination to determine memory B cell responses.

with 79 clones comprising half of all NK cells for P1 at 30 months, and 7 for P2 at 24 months (Fig. 5A). Quantitative digital droplet polymerase chain reaction (ddPCR) surveillance of the most abundant clones revealed the fluctuations in clonal abundance within each lineage (Fig. 5B). Although individual clones transiently increased in abundance, in particular those possessing integrations near the *TNFSF12* and the *PIM1* gene, these declined over time.

Vector integration site distribution

A comparison of P1's and P2's VISA data sets to an in vitro LV-transduced $CD34^{+}$ cell library data set (259,648 unique sites) mapped across the human genome (Fig. 6, and table S5) confirms LV's preferential targeting of actively expressed genes and gene-dense regions (79% within genes versus 39% for random control) (*24*, *25*) (discussed further in the Supplementary Materials and Methods). Also evident from this comparison is that the in vivo integration site repertoire is remarkably similar to that of the input clones, highlighting the dominant effect of the vector-specific integration preferences retained in in vivo patient samples independent of disease or therapeutic gene (WAS, MLD, and adrenoleukodystrophy) transferred (*12*, *13*). A comparison of shared integration sites between different lineages at different time points, or similarity index, shows highly variable integration site in myeloid cells, consistent with the increased cell turnover rates in myeloid compared with T cells (fig. S9).

Many of the integration sites in our patient samples are shared with the common integration sites (CIS) in the lentiviral WAS trial (*12*), although they do not appear to be enriched compared to the initial in vitro $CD34^{+}$ cell library, suggesting a lack of selective in vivo expansion. In contrast, *HMGA2* has multiple unique integrations, most of which are in the same orientation, especially in intron 3 (Fig. 5C). Although over 38-fold enrichment in *HMGA2* contribution is observed in vitro, the overall contribution from *HMGA2* integrant clones remained very low in all gene-marked cells (~1%), with no significant expansion of any single clone. In the β-thalassemia study, a single *HMGA2* integrant clone was highly expanded because of an alternative splice acceptor created by the unstable 2 × 250–bp cHS4 insulator core that resulted in the overexpression of a truncated and more stable *HMGA2* (high-mobility group AT-hook 2) protein (*29*). Using primers targeting the flanking insulators (fig. S10), we confirmed the integrity of our transgene sequence around the insulators, without any evidence for rearrangement. To assess for potential biological effects of the low-level expansion of *HMGA2* integrant clones, the expression level of *HMGA2* in different lineages of PB from P1 and P2 was determined using ddPCR assays for the 5′ (exon 3, before integration sites) and 3′ (exon 4/5, after integration site). Expression of *HMGA2* in all cell lineages was low (data not shown), and the

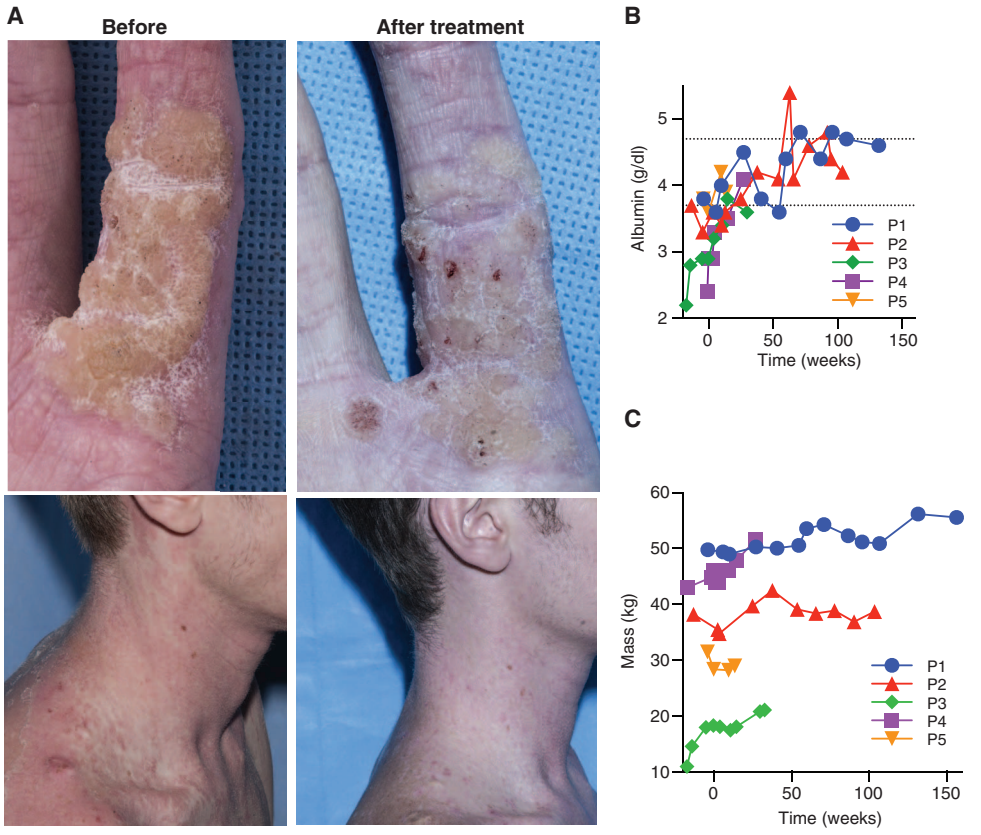

Fig. 4. Clinical progress after gene therapy. (**A**) Photographs demonstrating human papilloma virus warts (top) and molluscum contagiosum on P2 (bottom) before and 15 months after gene therapy as indicated. (**B**) Serial serum albumin for P1 to P5 after gene therapy. Upper and lower reference ranges are indicated by dotted lines. (**C**) Body mass measurements for P1 to P5 after treatment.

ratio of the 5′ assay/3′ assay was close to 1, suggesting no overexpression of a truncated form of *HMGA2*.

DISCUSSION

This study describes the first successful SIN-LV gene therapy with low-dose busulfan conditioning of older SCID-X1 patients who had failed previous HSCT. In P1 and P2, with ≥2-year follow-up, significant stable gene marking in multiple hematopoietic lineages coincided with reconstitution of humoral immunity, specific vaccine responses, and marked clinical improvement, in contrast to restricted T cell marking in prior mγRV gene therapy trials without conditioning (*4*). This was also the first use of SIN-LV made by a stable producer cell line, GPRG-γc, with multiple copies of SIN vector genomes generated by a concatemeric array transfection technique (*18*) that permitted production of high-titer vector (>10^8 iu/ml) sufficient to treat >1 × 10^9 or 2 × 10^7/kg cells for each patient (*17*). Despite reported improved outcomes with myeloid conditioning in ADA-SCID and WAS gene therapy trials, particularly with regard to B or NK cell reconstitution, no myeloconditioning has been used in SCID-X1 to date (*19*, *30*). Substantial multilineage marking in this study underscores the importance of myeloconditioning to improve engraftment in SCID-X1, although LV likely also targets HSCs more efficiently, because mγRV gene therapy with busulfan conditioning in CGD (*18*) and WAS (*19*) did not result in significant B cell gene marking.

Humoral reconstitution in P1 and P2 corresponded with the eradication of chronic norovirus in P1 and P2, a poorly appreciated medical problem in SCID-X1 patients with incomplete immune reconstitution after prior haploidentical HSCT without conditioning. Despite minimal diarrhea, chronic norovirus infection in these patients can result in a protein-losing enteropathy, electrolyte, mineral, and vitamin losses, and subsequent nutritional and growth failure with endoscopic appearance of celiac-like flat or blunted villi. It is interesting that the gene-corrected B cells were able to eradicate the norovirus, whereas both oral IgG (used by some to treat chronic norovirus) and intravenous IgG failed, suggesting a potentially unique role for gut lamina propria B cells in the control of norovirus.

We also report the first substantial gene marking and correction of NK cells in SCID-X1 after gene therapy with substantial clinical improvement of warts and molluscum (*31*). In contrast to the rapid expansion of gene-corrected T cells in SCID-X1 infants after gene therapy, the T cell marking in adult P1 and P2 increased slowly. Before gene therapy, P1 and P2 lacked donor stem cells, and together with the absence of TRECs, this suggests that circulating T cells were from a long-lived thymic population. The number of gene-corrected autologous cells continues to outcompete donor T cells as indicated by the T cell chimerism assays, and the increase in TRECs indicates the presence of at least some residual thymic function. Longer-term follow-up of similarly treated, but younger, SCID-X1 patients will shed light on the relative importance of a more preserved thymus. Of note, the increase of all lineages (T, B, and NK cells) continues steadily, and stable $CD34^+$ cell VCN even at 3 years after therapy (in P1) demonstrates the persistence of LV-corrected HSCs.

Quantitative ddPCR surveillance of specific clones revealed dynamic fluctuations in clonal contribution such as integrations near *PIM1*, *TNFSF12*, and *HMGA2*; *PIM1* transiently exceeded 20% of marked T cells but less than 4% of the total lineage. These clones decreased spontaneously over time. The integration profile in the patients is likely shaped by two major factors: first, the vector-preferred integration pattern at initial transduction, and second, the selective expansion in vivo. Most of the CIS identified in our study and in previous studies simply reflect the initial integration preference of LV, with no significant enrichment in vivo of any of the top CIS. With an in vitro CD34 integration data set as a reference baseline of input clones, in vivo clonal expansion determined by fold increase over in vitro sample revealed in vivo expansion of *HMGA2*, previously described in β-thalassemia

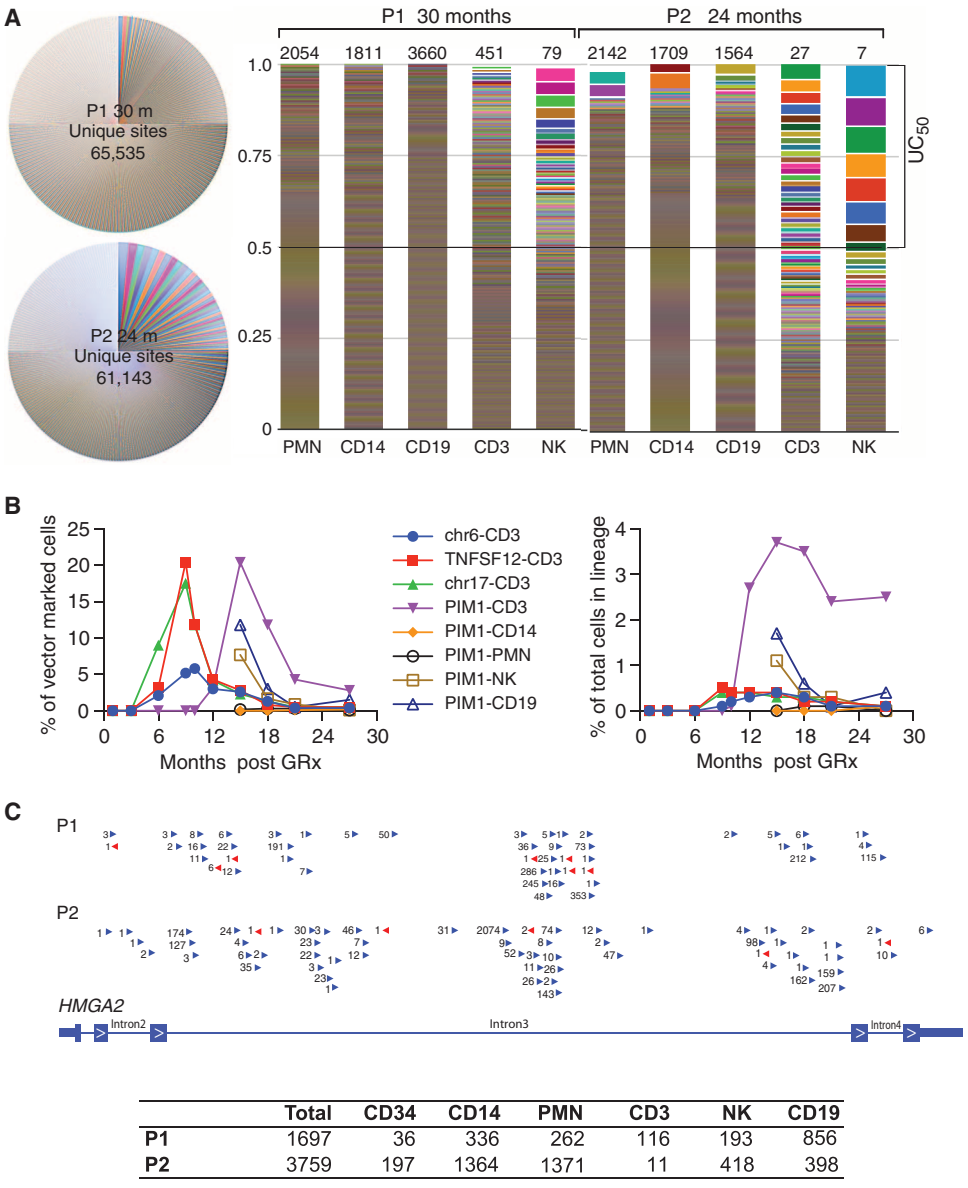

	Total	CD34	CD14	PMN	CD3	NK	CD19
P1	1697	36	336	262	116	193	856
P2	3759	197	1364	1371	11	418	398

Fig. 5. Vector integration site analysis. (**A**) Total unique integration sites, shown in proportion to their representation of the total diversity in P1 and P2 to 30 and 24 months (30 m, 24 m), respectively (left). Clonal composition for sorted cell lineages for P1 and P2 (right). Each horizontal bar represents clonal frequency, from most abundant on the top. The number of unique clones in the top 50% of the cells, UC_{50}, is listed above each sample. (**B**) Serial quantitative ddPCR tracking of the four most frequent clones [TNFSF12 (tumor necrosis factor ligand superfamily, member 12), TNFSF12-TNFSF13, chr6 (chromosome 6), and PIM1 (proto-oncogene serine/threonine-protein kinase)] in P2 is shown as a percentage of vector-marked cells (left) or of total cells in each lineage (right). GRx, gene therapy. (**C**) Schematic of unique integrations of *HMGA2* in P1 and P2. Most clones (enumerated next to the arrow) are in the same orientation as the gene (blue), with a few in the reverse orientation (red). Clones are seen in all lineages: CD34, CD14, CD19, NK and PMN, and CD3 (summarized below).

lentiviral gene therapy trial (*29*). Multiple independent integration sites in the *HMG2A* gene were found in both P1 and P2, but unlike the single *HMGA2* restricted to the myeloid lineage in the β-thalassemia trial, the *HMGA2* clones in P1 and P2 were present in all cell lineages (myeloid, T, B, and NK cells), suggesting the growth advantage occurred in stem cells. Furthermore, overexpression of the truncated *HMGA2* gene selectively occurred in erythroblasts but remained undetectable in granulocytes-monocytes despite presence of the same clone at a greater frequency (*29*). This suggests that the transcription of *HMGA2* gene is under tight regulation, with variable expression in specific cell types at specific time points. We hypothesize that the integrations in this study found in the *HMGA2* intron 3 transiently provide some growth advantage of host cells by production of the more stable truncated protein at a certain time point, but *HMGA2* gene remains under the control and regulation of its native promoters and can be turned off during the natural cell cycle or cell differentiation, which accounts for the absence of overexpression in P1 and P2 cells. The endogenous expression control for *HMGA2* gene likely limits the growth expansion influence from the *HMGA2* integration clones. Ongoing monitoring of *HMGA2* and other integration sites will shed further light on this.

Because SCID-X1 is a rare disease, a limitation of this study is the small number of patients treated. Furthermore, all patients have received prior haploidentical stem cell transplant that resulted in varying degrees of immune reconstitution. Consequently, the study population is heterogenous with a range of complex underlying medical problems that may impact the results. Although only the first two older patients have been observed up to 2 to 3 years, early myeloid gene marking corresponds to B cell gene marking and humoral immunity improvement, providing possible early indicators of outcome. Because vector-related mutagenesis did not appear until 3 to 4 years after gene therapy in the SCID-X1 infants (*22*), insertion-related mutagenesis cannot be definitively excluded, although the diverse repertoire of integrations to date, and the absence of adverse events in the larger experience with LV gene therapy in other diseases, is reassuring. Our results from the young adult patients suggest that LV-mediated gene therapy with reduced intensity conditioning is a promising approach for treatment of SCID-X1, including in older patients. Such interventions should be considered early to minimize irreversible organ damage from suboptimal immune reconstitution, because T cell reconstitution alone is clearly not sufficient to prevent or reverse progressive injury to lungs.

Fig. 6. Circular projection of the human genome with integration sites from P1 and P2 (in vivo, orange and red), in vitro LV-transduced CD34 cells (green), and in vitro mγRV-transduced CD34 cells (red). The top 100 target genes (in vitro) are listed on the outside, with the top 10 target genes (in vitro) in bold. MLV, murine leukemia virus.

MATERIALS AND METHODS

This is a phase 1/2 nonrandomized clinical trial of ex vivo HSC gene transfer treatment for SCID-X1 using a SIN, insulated LV. The study is approved by the National Institute of Allergy and Infectious Diseases (NIAID) Institutional Regulatory Board (clinical protocol #11-I-0007, ClinicalTrials.gov ID NCT01306019) and Institutional Biosafety Committee, FDA (investigational new drug #15041), sponsored by the NIAID Regulatory Compliance and Human Subjects Protection Branch.

Lentiviral vector

The Cl20-i4-EF1α-hγcOPT used in this clinical trial is the first use of LV produced by a previously described stable inducible LV producer cell line GPRTG (*15*, *18*). This is a vesicular stomatitis virus G (VSV-G)–pseudotyped, third-generation SIN vector that uses a promoter fragment from the eukaryotic EF1α gene to express a codon-optimized human γc cDNA and contains a 400-bp insulator fragment from the chicken β-globin locus within the SIN long terminal repeat (LTR). Large-scale clinical grade vector was manufactured at St. Jude Children's Research Hospital Vector Facility as previously published (*15*, *18*). Briefly, producer cells were cultured in WAVE Bioreactor System (GE Healthcare Biosciences), and harvests were filtered (Millipore), followed by a Mustang Q ion exchange (Pall) and a final concentration by diafiltration (Millipore) (*15*). Titers of the vector were 4.5 to 7.2 × 10^8 iu/ml.

Autologous CD34$^+$ HSCs collection and isolation

Patients receive G-CSF at 16 mg/kg per day by subcutaneous (sc) injection for five consecutive days, supplemented by plerixafor (0.24 mg/kg, sc, 11 hours before collection) [National Institutes of Health (NIH) protocol 94-I-0073] before apheresis at the NIH Clinical Center (*22*). The products were processed using FDA-approved Isolex immune anti-CD34 magnetic bead system to isolate and enrich CD34$^+$ cells by the NIH Department of Transfusion Medicine Cell Processing Facility. Purified CD34$^+$ HSCs were cryopreserved until gene therapy.

Transduction of CD34$^+$ HSCs

Ex vivo culture and transduction of the patient's autologous CD34$^+$ HSCs with VSV-G–pseudotyped Cl20-i4-EF1α-hγcOPT LV were performed and certified by the NIH Department of Transfusion Medicine Cell Processing Facility. Transduction involves thawing and suspension of patient CD34$^+$ HSCs in X-VIVO 10 serum-free growth medium [containing 1% human serum albumin plus cytokines (stem cell factor, 50 to 100 ng/ml; FLT-3L, 50 to 100 ng/ml; thrombopoietin, 50 to 100 ng/ml; IL-3, 5 ng/ml)]. The cells were cultured in T175 tissue culture flasks coated with the recombinant fibronectin fragment known as RetroNectin and exposed to LV for 6 to 8 hours each day for two consecutive days after an overnight prestimulation. Transduced CD34$^+$ HSCs were washed and infused over <30 min at the end of culture after required safety testing and quality control testing.

Conditioning regimen

A dose lower than that used in γRV gene therapy for CGD (10 mg/kg) (*18*) but higher than the dose used in γRV gene therapy for ADA (4 mg/kg) was chosen, at 6 mg/kg given over 2 days. The busulfan levels are shown in Table 1; no dose adjustment was given. No T cell– or B cell–depleting agents were given.

Clinical course

No adverse events were noted with the infusion of the transduced CD34$^+$ HSC cell product. The nadir for the expected busulfan-related effects of neutropenia and thrombocytopenia occurred at 2 to 3 weeks after treatment (fig. S2) and were recovered without requiring any cellular support or intervention. Subjects were discharged home by 3 to 4 weeks after gene therapy. Three of the five patients developed febrile neutropenia that responded to empiric antimicrobial therapy. An overview of the study implementation is shown in table S1.

Laboratory evaluation

Cell lineage separation for gene marking and integration analysis. After polymorphonuclear granulocyte (PMN) separation using Histopaque, the mononuclear leukocyte layer was fractionated by magnetic beads per manufacturer's instructions (Dynal Beads, Invitrogen) (Supplementary Materials and Methods). The purity of the bead-sorted PMN from a healthy donor was analyzed (fig. S3).

B cell preparations, flow cytometry phenotyping, and functional analyses. Immunophenotyping and cell sorting were performed on freshly processed PBMCs or PBMCs that had been cryopreserved with the following anti-human monoclonal antibodies: allophycocyanin (APC) anti-CD10, APC-H7 anti-CD20, and phycoerythrin (PE) anti-IgG (BD Biosciences); peridinin chlorophyll protein–Cy5.5 anti-CD19 and PE-Cy7 anti-CD27 (eBioscience); fluorescein isothiocyanate anti-CD21 (Beckman Coulter); VioBlue anti-IgA (Miltenyi Biotec); and Brilliant Violet 510 anti-IgM. Cell sorting and immunophenotyping were performed on BD FACSAria II and BD FACSCanto II (BD Biosciences) flow cytometers, respectively. Analyses were performed with FlowJo version 9.8.5 software (Tree Star). Memory B cell responses to influenza were performed by ELISpot as previously described (*23*), with B cells isolated by negative magnetic bead–based selection (STEMCELL Technologies). Phenotyping of immune cells by flow cytometry was also performed by the Clinical Laboratory Improvement Amendments–certified Clinical Immunology Laboratory/Department of Laboratory Medicine at the NIH Clinical Center.

B cell proliferation and class switching in response to IL21/CD40L. PBMCs of a healthy donor and P1 were labeled with CFSE (0.5 μM; Molecular Probes) and cultured with IL21 (50 ng/ml; PeproTech) and CD40L (500 ng/ml) (*24*–*26*). B cell proliferation was determined by CFSE dilution, and immunoglobulin class switch was measured by intracellular expression of IgG and IgM using flow cytometry.

Peripheral blood CD34$^+$ cell purification and expansion for VCN and integration site analyses. PBMCs were purified from non-mobilized peripheral blood by Ficoll separation (Lymphocyte Separation Medium, MP Biomedicals). CD34$^+$ cells were isolated from PBMCs using magnetic cell sorter magnetic beads (Miltenyi Biotec) according to the manufacturer's protocol. CD34$^+$ cells were expanded for 8 to 12 days in StemSpan II media (STEMCELL Technologies) supplemented with 100 ng/ml each of human stem cell factor, FLT-3L, and thrombopoietin (PeproTech). DNA was isolated using the DNeasy Blood and Tissue Kit (QIAGEN).

Quantitative determination of VCN by ddPCR. To measure the vector-carrying cells, we used a ddPCR (Bio-Rad) assay. The ddPCR assay allows the measurement of absolute copy number without using standard curve. The vector-specific primers and probes are as follows: HIV forward, 5′-CTGTTGTGTGACTCTGGTAACT-3′; HIV reverse, 5′-TTCGCTTTCAAGTCCCTGTT-3′; and HIV probe, 5′-/56-FAM/AAATCTCTA/ZEN/GCAGTGGCGCCCG/3IABkFQ/-3′. We multiplexed a reference gene assay for cell counts in the same reaction [myocardin-like protein 2 (MKL2): forward, 5′-AGATCAGAAGGGTGAGAAGAATG-3′; reverse, 5′-GGATGGTCTGGTAGTTGTAGTG-3′; and probe, 5′-/56-HEX/TGTTCCTGC/ZEN/AACTGCAGATCCTGA/3IABkFQ/-3′]. Cell number was calculated as half of the *MKL2* counts because each cell is diploid. VCN was calculated as vectors per cell.

Monitoring clonal expansion of specific integration site. Top expanded clones identified by the VISA sequencing assay were followed up and monitored by specific ddPCR assay. All of our ddPCR assays consist of a common LTR primer, an LTR probe, and a specific primer for genomic DNA junction [5LTR reverse, 5′-CTGCAGGGATCTTGTCTTCTT-3′; 5LTR junction probe, 5′-/56-FAM/TGGAAGGGC/ZEN/TAATTCACTCCCA/3IABkFQ/-3′; PIM1-5LTR primer, 5′-TCCTAACATCCCCACTGCAT-3′; TNFSF12-5LTR primer, 5′-ACAGTAAAGCAAGAGTGGGATG-3′; 3LTR forward, 5′-CCCACTGCTTAAGCCTCAATA-3′; 3LTR junction probe, 5′-/56-FAM/AAGTAGTGT/ZEN/GTGCCCGTCTGTTGT/3IABkFQ/-3′; CDKN1A (cyclin-dependent kinase inhibitor 1A)–3LTR primer, 5′-GCACGAAATCACTGCCATATTC-3′]. We multiplexed the integration site–specific assay together with the *MKL2* reference gene assay, which measures cell counts in the same reaction (*28*). The use of ddPCR makes it possible to (i) monitor the specific integration site accurately, (ii) use limited amount of input DNA, and (iii) make monitoring of expanded clones easy over time and across many different cell lineages.

Evaluation of insulator size in peripheral blood cells from P1

Genomic DNA P1 was used for PCR amplification; used PCR primer sequences for the 5′ LTR were 5′-CTGGAAGGGCTAATTCACTC-3′ (P1) and 5′-TCGCGATCTAATTCTCC-3′ (P2), and for the 3′ LTR were 5′-GCGGCCGCATCGATGCCGTATAC-3′ (P3) and 5′-CTGCTAGAGATTTTCCACAC-3′ (P4). The expected size of the 5′ and 3′ LTR PCR fragments with the intact 400-bp insulator element was 851 and 791 bp, respectively (the exact length of both LTRs is 649 bp without insulator). The sequences of the two PCR fragments were confirmed by direct DNA sequencing of the PCR product. The smaller band (around 500 bp) with the P1/P2 primer was TA-cloned and TA-sequenced, confirming a mispriming of P2 in the R region, which resulted in the artifact, and that the 400-bp insulator is intact.

SUPPLEMENTARY MATERIALS

www.sciencetranslationalmedicine.org/cgi/content/full/8/335/335ra57/DC1

Materials and Methods

Fig. S1. Summary of patient and product treatment.

Fig. S2. Surveillance of lymphocytes, platelets, and absolute neutrophil count to monitor effects of busulfan conditioning before cell infusion in patients (P1 to P5).

Fig. S3. Flow cytometric evaluation for CD3 T, CD19 B, and CD56 NK cells in purified PMN.

Fig. S4. Analysis of T cell receptor repertoire and TRECs.

Fig. S5. Absolute numbers of immune cells in subjects P3 to P5 after gene therapy.

Fig. S6. Class-switched memory B cells.

Fig. S7. NK cell phenotype.

Fig. S8. Chest computed tomography.

Fig. S9. Similarity index of vector integration sites.

Fig. S10. Vector insulator PCR.

Table S1. Protocol schedule for clinical procedures and follow-up.

Table S2. IS summary in P1 and P2.

Table S3. Combined IS from P1 up to 30m.
Table S4. Combined IS from P2 up to 24m.
Table S5. Lentivector integration sites in human CD34$^+$ cells in vitro, n = 259648.
Table S6. Comparison of in vitro and in vivo integration sites.
Table S7. Gene ontology KEGG PATHWAY.
References (*32*, *33*)

REFERENCES AND NOTES

1. M. D. Railey, Y. Lokhnygina, R. H. Buckley, Long-term clinical outcome of patients with severe combined immunodeficiency who received related donor bone marrow transplants without pretransplant chemotherapy or post-transplant GVHD prophylaxis. *J. Pediatr.* **155**, 834–840.e1 (2009).
2. B. Neven, S. Leroy, H. Decaluwe, F. Le Deist, C. Picard, D. Moshous, N. Mahlaoui, M. Debré, J.-L. Casanova, L. Dal Cortivo, Y. Madec, S. Hacein-Bey-Abina, G. de Saint Basile, J.-P. de Villartay, S. Blanche, M. Cavazzana-Calvo, A. Fischer, Long-term outcome after hematopoietic stem cell transplantation of a single-center cohort of 90 patients with severe combined immunodeficiency. *Blood* **113**, 4114–4124 (2009).
3. S. Y. Pai, B. R. Logan, L. M. Griffith, R. H. Buckley, R. E. Parrott, C. C. Dvorak, N. Kapoor, I. C. Hanson, A. H. Filipovich, S. Jyonouchi, K. E. Sullivan, T. N. Small, L. Burroughs, S. Skoda-Smith, A. E. Haight, A. Grizzle, M. A. Pulsipher, K. W. Chan, R. L. Fuleihan, E. Haddad, B. Loechelt, V. M. Aquino, A. Gillio, J. Davis, A. Knutsen, A. R. Smith, T. B. Moore, M. L. Schroeder, F. D. Goldman, J. A. Connelly, M. H. Porteus, Q. Xiang, W. T. Shearer, T. A. Fleisher, D. B. Kohn, J. M. Puck, L. D. Notarangelo, M. J. Cowan, R. J. O'Reilly, Transplantation outcomes for severe combined immunodeficiency, 2000–2009. *N. Engl. J. Med.* **371**, 434–446 (2014).
4. S. Hacein-Bey-Abina, J. Hauer, A. Lim, C. Picard, G. P. Wang, C. C. Berry, C. Martinache, F. Rieux-Laucat, S. Latour, B. H. Belohradsky, L. Leiva, R. Sorensen, M. Debré, J. Laurent Casanova, S. Blanche, A. Durandy, F. D. Bushman, A. Fischer, M. Cavazzana-Calvo, Efficacy of gene therapy for X-linked severe combined immunodeficiency. *N. Engl. J. Med.* **363**, 355–364 (2010).
5. J. Chinen, J. Davis, S. S. De Ravin, B. N. Hay, A. P. Hsu, G. F. Linton, N. Naumann, E. Y. H. Nomicos, C. Silvin, J. Ulrick, N. L. Whiting-Theobald, H. L. Malech, J. M. Puck, Gene therapy improves immune function in preadolescents with X-linked severe combined immunodeficiency. *Blood* **110**, 67–73 (2007).
6. A. J. Thrasher, S. Hacein-Bey-Abina, H. B. Gaspar, S. Blanche, E. G. Davies, K. Parsley, K. Gilmour, D. King, S. Howe, J. Sinclair, C. Hue, F. Carlier, C. von Kalle, G. de Saint Basile, F. le Deist, A. Fischer, M. Cavazzana-Calvo, Failure of SCID-X1 gene therapy in older patients. *Blood* **105**, 4255–4257 (2005).
7. M. G. Ott, M. Schmidt, K. Schwarzwaelder, S. Stein, U. Siler, U. Koehl, H. Glimm, K. Kühlcke, A. Schilz, H. Kunkel, S. Naundorf, A. Brinkmann, A. Deichmann, M. Fischer, C. Ball, I. Pilz, C. Dunbar, Y. Du, N. A. Jenkins, N. G. Copeland, U. Lüthi, M. Hassan, A. J. Thrasher, D. Hoelzer, C. von Kalle, R. Seger, M. Grez, Correction of X-linked chronic granulomatous disease by gene therapy, augmented by insertional activation of *MDS1-EVI1*, *PRDM16* or *SETBP1*. *Nat. Med.* **12**, 401–409 (2006).
8. S. J. Howe, M. R. Mansour, K. Schwarzwaelder, C. Bartholomae, M. Hubank, H. Kempski, M. H. Brugman, K. Pike-Overzet, S. J. Chatters, D. de Ridder, K. C. Gilmour, S. Adams, S. I. Thornhill, K. L. Parsley, F. J. T. Staal, R. E. Gale, D. C. Linch, J. Bayford, L. Brown, M. Quaye, C. Kinnon, P. Ancliff, D. K. Webb, M. Schmidt, C. von Kalle, H. B. Gaspar, A. J. Thrasher, Insertional mutagenesis combined with acquired somatic mutations causes leukemogenesis following gene therapy of SCID-X1 patients. *J. Clin. Invest.* **118**, 3143–3150 (2008).
9. A. Deichmann, S. Hacein-Bey-Abina, M. Schmidt, A. Garrigue, M. H. Brugman, J. Hu, H. Glimm, G. Gyapay, B. Prum, C. C. Fraser, N. Fischer, K. Schwarzwaelder, M.-L. Siegler, D. de Ridder, K. Pike-Overzet, S. J. Howe, A. J. Thrasher, G. Wagemaker, U. Abel, F. J. T. Staal, E. Delabesse, J.-L. Villeval, B. Aronow, C. Hue, C. Prinz, M. Wissler, C. Klanke, J. Weissenbach, I. Alexander, A. Fischer, C. von Kalle, M. Cavazzana-Calvo, Vector integration is nonrandom and clustered and influences the fate of lymphopoiesis in SCID-X1 gene therapy. *J. Clin. Invest.* **117**, 2225–2232 (2007).
10. S. Hacein-Bey-Abina, C. Von Kalle, M. Schmidt, M. P. McCormack, N. Wulffraat, P. Leboulch, A. Lim, C. S. Osborne, R. Pawliuk, E. Morillon, R. Sorensen, A. Forster, P. Fraser, J. I. Cohen, G. de Saint Basile, I. Alexander, U. Wintergerst, T. Frebourg, A. Aurias, D. Stoppa-Lyonnet, S. Romana, I. Radford-Weiss, F. Gross, F. Valensi, E. Delabesse, E. Macintyre, F. Sigaux, J. Soulier, L. E. Leiva, M. Wissler, C. Prinz, T. H. Rabbitts, F. Le Deist, A. Fischer, M. Cavazzana-Calvo, *LMO2*-associated clonal T cell proliferation in two patients after gene therapy for SCID-X1. *Science* **302**, 415–419 (2003).
11. S. Hacein-Bey-Abina, S.-Y. Pai, H. B. Gaspar, M. Armant, C. C. Berry, S. Blanche, J. Bleesing, J. Blondeau, H. de Boer, K. F. Buckland, L. Caccavelli, G. Cros, S. De Oliveira, K. S. Fernández, D. Guo, C. E. Harris, G. Hopkins, L. E. Lehmann, A. Lim, W. B. London, J. C. M. van der Loo, N. Malani, F. Male, P. Malik, M. A. Marinovic, A.-M. McNicol, D. Moshous, B. Neven, M. Oleastro, C. Picard, J. Ritz, C. Rivat, A. Schambach, K. L. Shaw, E. A. Sherman, L. E. Silberstein, E. Six, F. Touzot, A. Tsytsykova, J. Xu-Bayford, C. Baum, F. D. Bushman, A. Fischer, D. B. Kohn, A. H. Filipovich, L. D. Notarangelo, M. Cavazzana, D. A. Williams, A. J. Thrasher, A modified γ-retrovirus vector for X-linked severe combined immunodeficiency. *N. Engl. J. Med.* **371**, 1407–1417 (2014).
12. A. Aiuti, L. Biasco, S. Scaramuzza, F. Ferrua, M. P. Cicalese, C. Baricordi, F. Dionisio, A. Calabria, S. Giannelli, M. C. Castiello, M. Bosticardo, C. Evangelio, A. Assanelli, M. Casiraghi, S. Di Nunzio, L. Callegaro, C. Benati, P. Rizzardi, D. Pellin, C. Di Serio, M. Schmidt, C. Von Kalle, J. Gardner, N. Mehta, V. Neduva, D. J. Dow, A. Galy, R. Miniero, A. Finocchi, A. Metin, P. P. Banerjee, J. S. Orange, S. Galimberti, M. G. Valsecchi, A. Biffi, E. Montini, A. Villa, F. Ciceri, M. G. Roncarolo, L. Naldini, Lentiviral hematopoietic stem cell gene therapy in patients with Wiskott-Aldrich syndrome. *Science* **341**, 1233151 (2013).
13. A. Biffi, E. Montini, L. Lorioli, M. Cesani, F. Fumagalli, T. Plati, C. Baldoli, S. Martino, A. Calabria, S. Canale, F. Benedicenti, G. Vallanti, L. Biasco, S. Leo, N. Kabbara, G. Zanetti, W. B. Rizzo, N. A. Mehta, M. P. Cicalese, M. Casiraghi, J. J. Boelens, U. Del Carro, D. J. Dow, M. Schmidt, A. Assanelli, V. Neduva, C. Di Serio, E. Stupka, J. Gardner, C. von Kalle, C. Bordignon, F. Ciceri, A. Rovelli, M. G. Roncarolo, A. Aiuti, M. Sessa, L. Naldini, Lentiviral hematopoietic stem cell gene therapy benefits metachromatic leukodystrophy. *Science* **341**, 1233158 (2013).
14. S. Zhou, D. Mody, S. S. DeRavin, J. Hauer, T. Lu, Z. Ma, S. Hacein-Bey Abina, J. T. Gray, M. R. Greene, M. Cavazzana-Calvo, H. L. Malech, B. P. Sorrentino, A self-inactivating lentiviral vector for SCID-X1 gene therapy that does not activate LMO2 expression in human T cells. *Blood* **116**, 900–908 (2010).
15. M. R. Greene, T. Lockey, P. K. Mehta, Y.-S. Kim, P. W. Eldridge, J. T. Gray, B. P. Sorrentino, Transduction of human CD34$^+$ repopulating cells with a self-inactivating lentiviral vector for SCID-X1 produced at clinical scale by a stable cell line. *Hum. Gene Ther. Methods* **23**, 297–308 (2012).
16. S. Zhou, Z. Ma, T. Lu, L. Janke, J. T. Gray, B. P. Sorrentino, Mouse transplant models for evaluating the oncogenic risk of a self-inactivating XSCID lentiviral vector. *PLOS One* **8**, e62333 (2013).
17. S. Zhou, D. Mody, S. S. DeRavin, J. Hauer, T. Lu, Z. Ma, S. Hacein-Bey Abina, J. T. Gray, M. R. Greene, M. Cavazzana-Calvo, H. L. Malech, B. P. Sorrentino, A self-inactivating lentiviral vector for SCID-X1 gene therapy that does not activate LMO2 expression in human T cells. *Blood* **116**, 900–908 (2010).
18. R. E. Throm, A. A. Ouma, S. Zhou, A. Chandrasekaran, T. Lockey, M. Greene, S. S. De Ravin, M. Moayeri, H. L. Malech, B. P. Sorrentino, J. T. Gray, Efficient construction of producer cell lines for a SIN lentiviral vector for SCID-X1 gene therapy by concatemeric array transfection. *Blood* **113**, 5104–5110 (2009).
19. F. Candotti, K. L. Shaw, L. Muul, D. Carbonaro, R. Sokolic, C. Choi, S. H. Schurman, E. Garabedian, C. Kesserwan, G. J. Jagadeesh, P.-Y. Fu, E. Gschweng, A. Cooper, J. F. Tisdale, K. I. Weinberg, G. M. Crooks, N. Kapoor, A. Shah, H. Abdel-Azim, X.-J. Yu, M. Smogorzewska, A. S. Wayne, H. M. Rosenblatt, C. M. Davis, C. Hanson, R. G. Rishi, X. Wang, D. Gjertson, O. O. Yang, A. Balamurugan, G. Bauer, J. A. Ireland, B. C. Engel, G. M. Podsakoff, M. S. Hershfield, R. M. Blaese, R. Parkman, D. B. Kohn, Gene therapy for adenosine deaminase-deficient severe combined immune deficiency: Clinical comparison of retroviral vectors and treatment plans. *Blood* **120**, 3635–3646 (2012).
20. A. Aiuti, I. Brigida, F. Ferrua, B. Cappelli, R. Chiesa, S. Marktel, M.-G. Roncarolo, Hematopoietic stem cell gene therapy for adenosine deaminase deficient-SCID. *Immunol. Res.* **44**, 150–159 (2009).
21. S. R. Panch, Y. Y. Yau, E. M. Kang, S. S. De Ravin, H. L. Malech, S. F. Leitman, Mobilization characteristics and strategies to improve hematopoietic progenitor cell mobilization and collection in patients with chronic granulomatous disease and severe combined immunodeficiency. *Transfusion* **55**, 265–274 (2015).
22. S. Hacein-Bey-Abina, C. von Kalle, M. Schmidt, F. Le Deist, N. Wulffraat, E. McIntyre, I. Radford, J.-L. Villeval, C. C. Fraser, M. Cavazzana-Calvo, A. Fischer, A serious adverse event after successful gene therapy for X-linked severe combined immunodeficiency. *N. Engl. J. Med.* **348**, 255–256 (2003).
23. S. Suryani, D. A. Fulcher, B. Santner-Nanan, R. Nanan, M. Wong, P. J. Shaw, J. Gibson, A. Williams, S. G. Tangye, Differential expression of CD21 identifies developmentally and functionally distinct subsets of human transitional B cells. *Blood* **115**, 519–529 (2010).
24. X. Wu, Y. Li, B. Crise, S. M. Burgess, Transcription start regions in the human genome are favored targets for MLV integration. *Science* **300**, 1749–1751 (2003).
25. S. S. De Ravin, L. Su, N. Theobald, U. Choi, J. L. Macpherson, M. Poidinger, G. Symonds, S. M. Pond, A. L. Ferris, S. H. Hughes, H. L. Malech, X. Wu, Enhancers are major targets for murine leukemia virus vector integration. *J. Virol.* **88**, 4504–4513 (2014).
26. A. Chao, Nonparametric estimation of the number of classes in a population. *Scand. J. Statist.* **11**, 265–270 (1984).
27. N. A. Gillet, N. Malani, A. Melamed, N. Gormley, R. Carter, D. Bentley, C. Berry, F. D. Bushman, G. P. Taylor, C. R. M. Bangham, The host genomic environment of the provirus determines the abundance of HTLV-1–infected T-cell clones. *Blood* **117**, 3113–3122 (2011).
28. F. Maldarelli, X. Wu, L. Su, F. R. Simonetti, W. Shao, S. Hill, J. Spindler, A. L. Ferris, J. W. Mellors, M. F. Kearney, J. M. Coffin, S. H. Hughes, HIV latency. Specific HIV integration sites are linked to clonal expansion and persistence of infected cells. *Science* **345**, 179–183 (2014).

29. M. Cavazzana-Calvo, E. Payen, O. Negre, G. Wang, K. Hehir, F. Fusil, J. Down, M. Denaro, T. Brady, K. Westerman, R. Cavallesco, B. Gillet-Legrand, L. Caccavelli, R. Sgarra, L. Maouche-Chrétien, F. Bernaudin, R. Girot, R. Dorazio, G. J. Mulder, A. Polack, A. Bank, J. Soulier, J. Larghero, N. Kabbara, B. Dalle, B. Gourmel, G. Socie, S. Chrétien, N. Cartier, P. Aubourg, A. Fischer, K. Cornetta, F. Galacteros, Y. Beuzard, E. Gluckman, F. Bushman, S. Hacein-Bey-Abina, P. Leboulch, Transfusion independence and HMGA2 activation after gene therapy of human β-thalassaemia. *Nature* **467**, 318–322 (2010).
30. A. Aiuti, F. Cattaneo, S. Galimberti, U. Benninghoff, B. Cassani, L. Callegaro, S. Scaramuzza, G. Andolfi, M. Mirolo, I. Brigida, A. Tabucchi, F. Carlucci, M. Eibl, M. Aker, S. Slavin, H. Al-Mousa, A. Al Ghonaium, A. Ferster, A. Duppenthaler, L. Notarangelo, U. Wintergerst, R. H. Buckley, M. Bregni, S. Marktel, M. G. Valsecchi, P. Rossi, F. Ciceri, R. Miniero, C. Bordignon, M.-G. Roncarolo, Gene therapy for immunodeficiency due to adenosine deaminase deficiency. *N. Engl. J. Med.* **360**, 447–458 (2009).
31. Q. U. A. Kamili, F. O. Seeborg, K. Saxena, S. K. Nicholas, P. P. Banerjee, L. S. Angelo, E. M. Mace, L. R. Forbes, C. Martinez, T. S. Wright, J. S. Orange, I. C. Hanson, Severe cutaneous human papillomavirus infection associated with natural killer cell deficiency following stem cell transplantation for severe combined immunodeficiency. *J. Allergy Clin. Immunol.* **134**, 1451–1453.e1 (2014).
32. D. W. Huang, B. T. Sherman, R. A. Lempicki, Systematic and integrative analysis of large gene lists using DAVID bioinformatics resources. *Nat. Protoc.* **4**, 44–57 (2009).
33. D. W. Huang, B. T. Sherman, R. A. Lempicki, Bioinformatics enrichment tools: Paths toward the comprehensive functional analysis of large gene lists. *Nucleic Acids Res.* **37**, 1–13 (2009).

Acknowledgments: We dedicate this manuscript to the memory of D. Persons, who generated the CI20 series LV backbone used to construct the specific vector used in this trial. He was a friend and inspiration to us all. We also thank members of the Cell Processing Unit and Dowling Apheresis Unit, Department of Transfusion Medicine at the NIH Clinical Center, for apheresis of $CD34^+$ stem cells and the transduction of the cell products for this study. We also thank members of the Neutrophil Monitoring Laboratory at Leidos Biomedical Ltd. for preparing and archiving patient samples. Finally, we thank our Laboratory of Host Defenses clinical support team, as well as our patients and their families. **Funding:** This research was supported by the Intramural Research Program of NIAID, NIH (intramural project numbers Z01-A1-00644 and Z01-A1-00988), and the National Heart, Lung, and Blood Institute (grant P01HL 53749) and NIH-NIAID Grant U54 AI 082973. This project has been funded in part with federal funds from the Frederick National Laboratory for Cancer Research, NIH, under contract HHSN261200800001E (X.W. and L.S.), and the ASSISI Foundation of Memphis. The content of this publication does not necessarily reflect the views or policies of the Department of Health and Human Services nor does the mention of trade names, commercial products, or organizations imply endorsement by the U.S. Government. Replication-competent viruses assay was performed by the National Gene Vector Biorepository, Indiana University. **Author contributions:** S.S.D.R., H.L.M., S.A.O., N.K., J.U., P.L., M. Marquesen, and D.H. conducted the clinical study; X.W., S.M., L.K., C.M.B., G.O., D.M., D.K., L.S., N.T., U.C., and J.L. performed the experiments; R.E.T., S.Z., M. Meagher, B.P.S., J.T.G., S.S.D.R., U.C., and H.L.M. developed vector and novel stable cell line; L.D.N., I.C.H., M.J.C., E.K., and C.H. contributed to patient care; and S.S.D.R., K.A.Z., X.W., and H.L.M. analyzed the data and wrote the manuscript. **Competing interests:** J.T.G. is currently an employee of Audentes Ltd. All other authors declare that they have no competing interests. **Data and materials availability:** Materials described here will be provided upon request and execution of a material transfer agreement with NIAID, NIH, and/or St. Jude Children's Research Hospital.

Submitted 16 November 2015
Accepted 3 March 2016
Published 20 April 2016
10.1126/scitranslmed.aad8856

Citation: S. S. De Ravin, X. Wu, S. Moir, L. Kardava, S. Anaya-O'Brien, N. Kwatemaa, P. Littel, N. Theobald, U. Choi, L. Su, M. Marquesen, D. Hilligoss, J. Lee, C. M. Buckner, K. A. Zarember, G. O'Connor, D. McVicar, D. Kuhns, R. E. Throm, S. Zhou, L. D. Notarangelo, I. C. Hanson, M. J. Cowan, E. Kang, C. Hadigan, M. Meagher, J. T. Gray, B. P. Sorrentino, H. L. Malech, Lentiviral hematopoietic stem cell gene therapy for X-linked severe combined immunodeficiency. *Sci. Transl. Med.* **8**, 335ra57 (2016).

Science Translational Medicine
AAAS

Lentiviral hematopoietic stem cell gene therapy for X-linked severe combined immunodeficiency

Suk See De Ravin, Xiaolin Wu, Susan Moir, Lela Kardava, Sandra Anaya-O'Brien, Nana Kwatemaa, Patricia Littel, Narda Theobald, Uimook Choi, Ling Su, Martha Marquesen, Dianne Hilligoss, Janet Lee, Clarissa M. Buckner, Kol A. Zarember, Geraldine O'Connor, Daniel McVicar, Douglas Kuhns, Robert E. Throm, Sheng Zhou, Luigi D. Notarangelo, I. Celine Hanson, Mort J. Cowan, Elizabeth Kang, Coleen Hadigan, Michael Meagher, John T. Gray, Brian P. Sorrentino and Harry L. Malech (April 20, 2016)

Science Translational Medicine **8** (335), 335ra57. [doi: 10.1126/scitranslmed.aad8856]

Editor's Summary

SCID gene therapy comes of age

Diseases caused by mutations in single genes are prime candidates for gene therapy. X-linked severe combined immunodeficiency (SCID-X1) patients have mutations in *IL2RG*, which encodes the common γ chain of several interleukin receptors, resulting in lack of adaptive immune cells. Gene therapy has shown promise in SCID infants but failed in older SCID-X1 children. Now, De Ravin *et al*. report that lentiviral gene therapy with nonmyeloablative conditioning corrected multiple immune cell types in five older SCID-X1 patients whose symptoms persisted despite undergoing hematopoietic stem cell transplant(s) as infants. Humoral immunity restoration with normal immunoglobulin production and responses to immunization is confirmed in the first two patients with longer follow-up.

Science Translational Medicine (print ISSN 1946-6234; online ISSN 1946-6242) is published weekly, except the last week in December, by the American Association for the Advancement of Science, 1200 New York Avenue, NW, Washington, DC 20005.

Science Translational Medicine (print ISSN 1946-6234; online ISSN 1946-6242) is published weekly, except the last week in December, by the American Association for the Advancement of Science, 1200 New York Avenue, NW, Washington, DC 20005.